Mustansiriyah Journal of Pure and Applied Sciences

www.MJPAS.com

Hyperthermia Efficiency of Hydrothermal Synthesized Iron Sulfide Magnetic Nanoparticles

Mustafa Shakir Hashim 1* , Dalal Maseer Naser [2] , Sadiq H. Lafta [3]

[1,2] Physics department, Education College, Mustansiriyah University, Baghdad, Iraq : mustmust@uomustansiriyah.edu.iq. Orcid: 0000-0002-0085-6795.[1] , dallalnasser74@uomustansiriyah.edu.iq. Orcid: 0009-0007-9506-7521[2]

[3] Applied Sciences Department, University of Technology, Baghdad-Iraq : sadeq.h.lafta@uotechnology.edu.iq. Orcid: 0000-0002-7000-8337.[3]

A B S T R A C T

The hydrothermal technique was used to prepare iron sulfide magnetic nanoparticles using $FeCl_3 \cdot 6H_2O$, thiourea, and ethylene glycol as precursors. The hydrothermal process was accomplished on a hot plate at 320°C for 18 hours. X-ray diffraction (XRD) confirmed the production of iron sulfide with three phases. The dominant phase was (Fe_3S_4) greigite (67%) having a saturation magnetization of 9.1 emu/g. Scanning electron microscope (SEM) images approved the creation of nanoparticles with a mean diameter of 36.24nm. Alternating coil current amplitude of 100A and the frequency of about 100kHz were exerted on the sample to accomplish the hyperthermia test. Using a shallow concentration of magnetic nanoparticles, 20µg in 1.5ml of distilled water, produced a specific loss power (SLP) of about 3548 W/g. The produced particle sizes were suitable for producing good SLP value compared to the literature due to their magnetic hysteresis loss.

Keywords: Hyperthermia, Greigite, nanoparticles, specific loss power

1. Introduction

Nanomaterials have become an increasingly popular choice in biotherapeutic research for a variety of diseases, particularly in cancer treatment, due to their non-invasive and safe nature [1]. Magnetic nanoparticles (MNPs) have exceptional properties and applications in various fields, including environment, biomedicine, and clinical domains [2,3]. They are widely used for target-specific drug delivery, acting as contrast agents in magnetic resonance imaging, treating hyperthermia, and disease detection sensors[4]. MNPs have various uses

*Corresponding author : Mustafa Shakir Hashim
E-mail address: mustmust@uomustansiriyah.edu.iq.[1] ,

and can be customized in size, shape, composition, and surface properties. The characteristics of substances can change as particle size is reduced to the nano range [5]. However, because of the high surface energy, controlling particle size is difficult.

Since iron-based sulfides exhibit magnetic characteristics, much study has been done on them. They have been used in a number of industries, including biosensors, photodetectors, magnetothermal treatment, and magnetic resonance imaging. These materials' size, shape, and composition all affect how well they operate magnetically. Furthermore, there is a clear correlation between their magnetic characteristics and crystallinity [6]. Such nanoparticles are commonly synthesized via hydrothermal synthesis, coprecipitation, and thermal breakdown [7].

MNPs show great promise as a cancer treatment modality [8]. They function by inflicting mechanical and thermal damage, the latter of which can happen via three different processes to eliminate cancer cells: Hysteresis, Brownian, and Neel loss [9]. The best method for specifically harming cancer cells while causing the least amount of damage to healthy cells is hysteresis loss [10].

The formation of crystalline phases is particularly benefited by the hydrothermal process. Additionally, it permits the production of magnetic nanoparticles with high vapor pressure at melting temperatures while retaining the highest level of precision in composition control [11]. To achieve high temperatures and pressures, high-pressure reactors or autoclaves are specifically used in the hydrothermal technique and solvothermal synthesis. To stop the dislocation formation in single-crystal magnetic nanoparticles, this method uses aqueous or non-aqueous solutions at high pressures and temperatures [12].

Because of its high productivity and ease of use, the hydrothermal synthesis process is widely used in laboratory and industrial settings. This approach has been successfully used to synthesis a variety of iron-based sulfides, such as FeS_2 microspheres, metastable FeS_2, FeS_2 quantum dots, FeS nanosheets, FeS nanodots, Fe_3S_4 microspheres, and Fe_3S_4 nanoflowers. [13].

Magnetic hyperthermia (MH) is a therapy that heats tissue using magnetic nanoparticles and alternating magnetic fields [14]. MH method offers a range of benefits, including non-invasiveness, remote controllability, molecular-level specificity, unlimited penetration depth, and nanoscale spatial resolution. However, there are some limitations to this technique, such as the relatively low specific heating power, which may require a larger quantity of nanoparticles[15].

MH technique generates heat in a medium containing specific geometric and structural magnetic nanoparticles when exposed to alternating magnetic fields. This technique raises the temperature of cancer cells without affecting surrounding healthy cells by inducing apoptosis at a temperature range of 41-46°C for a brief period. Tumor cells have lower pH levels, which makes them more susceptible to overheating, while the poor blood supply to the tumor cells hinders heat dissipation. The use of MH for biomedical purposes was recently proposed and holds great potential in the field of medicine as long as the magnetic field and frequency

do not exceed the biological safety limits to avoid damage for healthy cells and tissues [10,16].

The frequency and intensity of the magnetic field affect the amount of heat produced. The specific absorption rate (SAR) (W/g), which is a function of the material composition and its micro-structural features (material type, particle size, size distribution, shape, dipolar interaction, surface functionalization, etc.), determines the heating capacity of nanoparticles. The efficacy of the heating is controlled by modifying these characteristics [17].

The magnetic heating efficiency of MNPs is generally evaluated by SAR or their equivalent parameters-specific loss power (SLP), [18,19], as seen in equations (1) and (2):

$$\mathrm{SAR} = \frac{\triangle \mathrm{T}}{\triangle \mathrm{t}} \quad \frac{\mathrm{c}}{m_{\mathrm{fe}}} \tag{1}$$

$$SLP = \frac{\triangle \mathrm{T}}{\triangle \mathrm{t}} \frac{\mathrm{c}}{m/V_s} \tag{2}$$

where c is the volumetric specific heat capacity of the solution, m_{fe} is the mass concentration of magnetic element in the solution, m is the mass of magnetic element in the solution, V_s is the sample volume, and t is time. Calorimetry is a straightforward technique for measuring the amount of heat and determining SAR. Based on the measurement of the temperature evolution of the target sample, heat quantification can be achieved [10].

It has been revealed that Fe_3S_4 nanoparticles have a very good magnetocaloric effect which could be used in magnetic hyperthermia for deep thrombosis [20].

The purpose of this work is to check the response of iron sulfide with high concentration of Fe_3S_4 to the applied AC magnetic field to raise its temperature in an aqueous solution to be a candidate solution for hyperthermia treatment.

Experimental part:

The precursor materials were FeCl3·6H2O (98%) as provided by FLUKA Chemicals Ltd, thiourea (>98%), and ethylene glycol (99.5%) as purchased from Gpr Chem Pvt Ltd. At first, a solution of FeCl3·6H2O (4mmol) and thiourea (8mmol) was mixed with 20ml of deionized water and 40ml of ethylene glycol. This was followed by stirring the precursor solution for 30 minutes until it became homogeneous. The resulting mixture was then placed into a sealed Teflon-lined stainless steel container, and heated on a hot plate at 320°C for 18 hours. The mentioned temperature was read from the built-in thermocouple on the surface of the hotplate while the temperature outside the middle of the autoclave was 180^{o}C. After cooling down to room temperature, the black powder that formed was filtered using the magnetic decantation method. The filtered powder was then washed several times with water and ethanol. The product was subsequently dried at 60°C for 3 hours in a vacuum oven for further characterization purposes. The sample was analyzed using the Shimadzu 6000 X-ray diffractometer using the source Cu-kα at λ=1.5406Å, operating at 40 kV and 30mA to accomplish the X-ray diffraction test (XRD). The field emission scanning electron

microscope (FESEM) MIRA3 TESCAN, the French model, was used for SEM analysis. The vibrating sample magnetometer (VSM)) device, model MDK, was utilized to measure the hysteresis loop curve and magnetic properties. The measurement was made at room temperature at a scan speed (step) of 0.05step/sec.

To perform the hyperthermia test, a sample weight, 20µg, of iron sulfide was placed in 1.5ml water within a plastic tube inside a helical copper pipe coil cooled by water. The coil dimensions were 2.5cm inner diameter, 7cm hight, and involving 7turns. The coil was lined by a glass wool to perform the insulation from external Undesirable heating. An electric circuit provides an AC power characterized by 100 kHz radio frequency, 100A for the current amplitude and about 1000W power to the copper coil as a hyperthermia system. The resulting temperature was monitored using a non-contact digital IR infrared thermometer with laser guide, type EQ-DT8530 IR- Thermometer. The temperature was recorded about each 1min. Fig.(1) shows a simplified diagram of the hyperthermia setup.

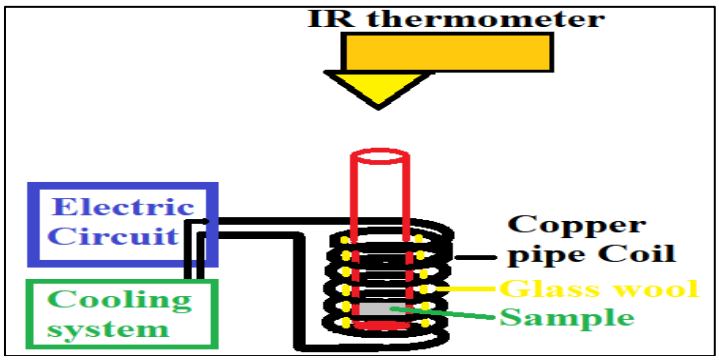

Fig.(1). The setting of the used hyperthermia.

Results and discussion

XRD analysis revealed the presence of three phases of iron sulfide, see Fig.(2).

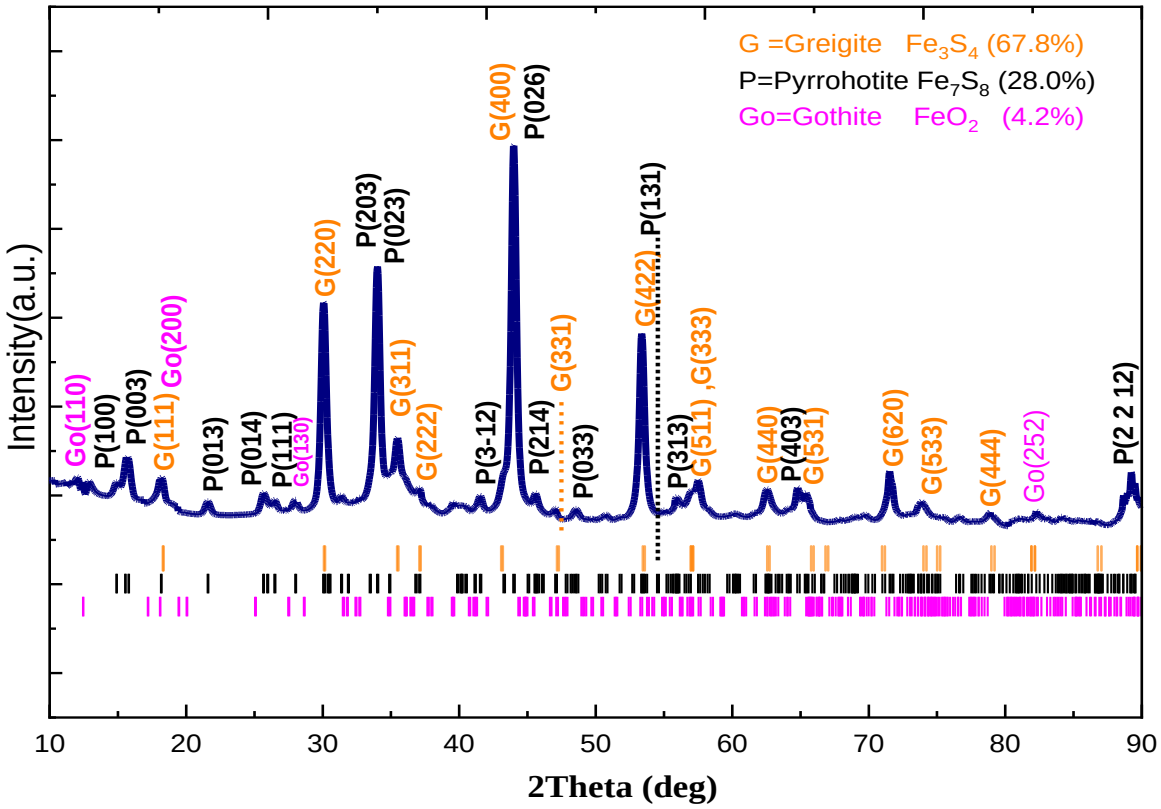

Fig.(2). The XRD pattern of the synthesized iron sulfide nanoparticles using hydrothermal conditions of 315°C for 18h.

The first phase was identified as greigite (Fe_3S_4) with a cubic crystal structure and a spinel-type arrangement (space group Fd3m). Four strong peaks at 30.12°, 35.52°, 62.57°and 71.18° were observed for greigite. The second identified phase was the pyrrhotite (Fe_7S_8), which has a trigonal crystal structure (space group: P31). Four strong peaks, which are 33.98°, 53.47°, 62.43° and 44.04°, are belonging to Fe_7S_8 in the pattern. The third phase was goethite (FeO_2) with the orthorhombic crystal structure (space group Pbnm) owning the peak diffraction peaks at 21.24°, and 65.48°. The Rietveld refinement for the produced pattern showed that the dominant phase was greigite at 67.8%, while the Fe_7S_8 at 28% and FeO_2 at 4.2%. The card numbers of the appeared phases in fig.2 are Fe_3S_4(COD #9000123), Fe_7S_8(COD #2106197), and FeO_2(COD #9011412).

Based on the literature, it was found that the formation of the Fe_3S_4 phase occurred due to a phase transition of pyrite at a temperature below 200°C [21]. At a temperature of 315°C, the phase transition from Fe_3S4 to pyrrhotite (Fe_7S_8) takes place. Yan-Hong Chen and his colleagues reported that at around 320°C, greigite gradually transforms into pyrite and pyrrhotite [22].

Fig.(3) illustrates the FESEM images of the prepared sample. The shape of the nanoparticles produced is irregular and they tend to agglomerate and form micro-aggregates. The average particle size was 36nm, where the sizes of the particles extended from 15nm to 75nm, involving a high concentration of around 35nm, as shown in Fig.(3)c.

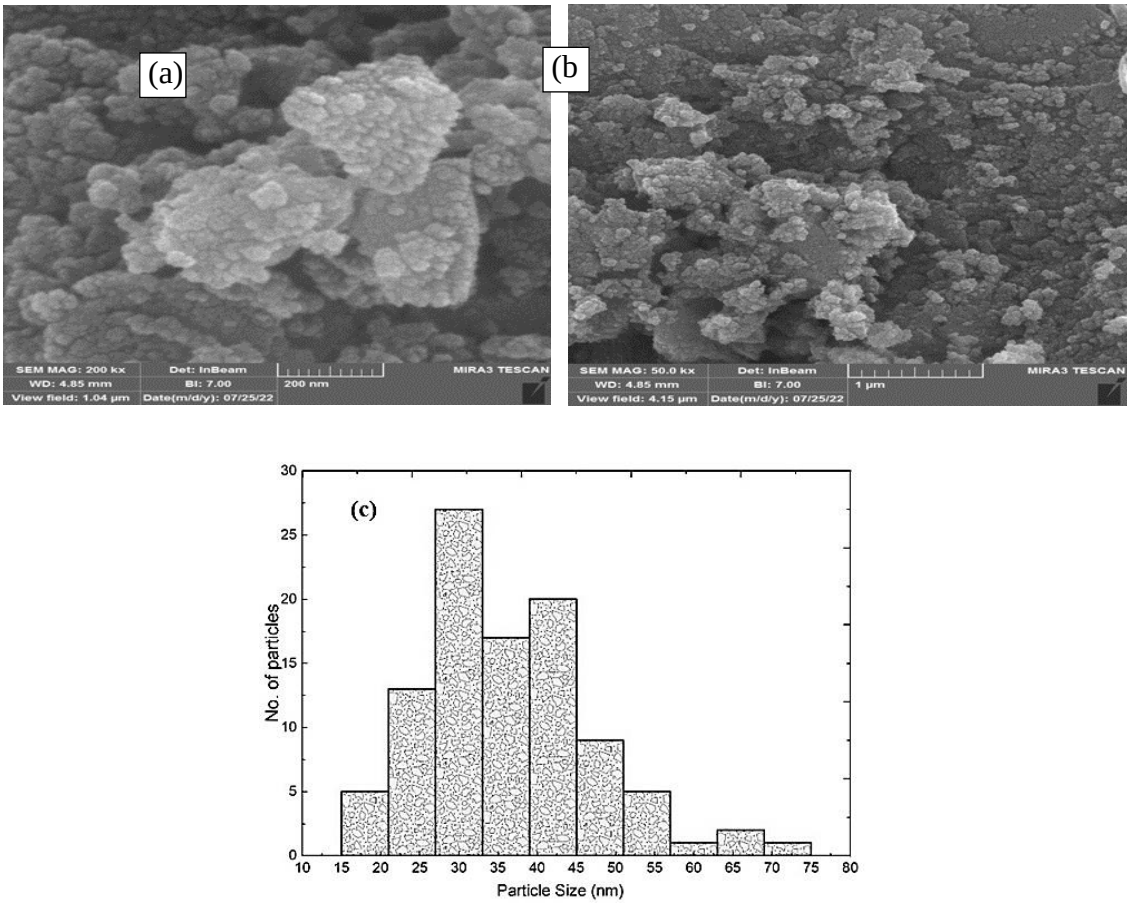

Fig.(3).FESEM images, (a) and (b), of the prepared nanoparticles, at magnification of 200kx and 50kx.

Fig.(4) shows the magnetic hysteresis loop of the prepared iron sulfide sample. The magnetic hysteresis loop associated magnetic parameters and some structural properties are listed in Table1.

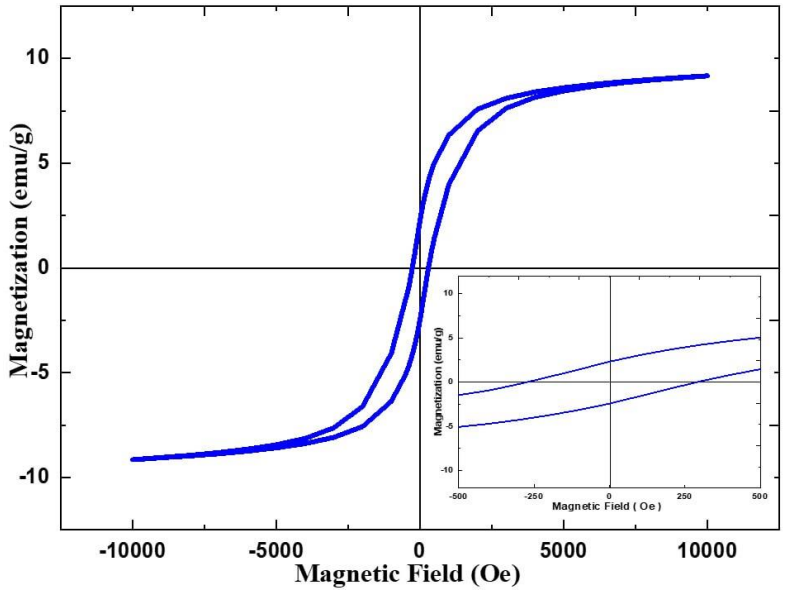

Fig.(4). Hysteresis loop of the prepared iron sulfide nanoparticles at 300^{0}K. The inset illustrates the intercepts of the loop with axes.

Table1.Magnetic parameters, particle size and crystallite size of the prepared iron sulfide nanoparticles.

M_s (emu/g)	M_r (emu/g)	H_c (Oe)	Particle size (nm)	Crystallite size (nm)
9.1	2.4	245	36.24	19

The magnetic hysteresis loop of the sample exhibits a normal ferrimagnetic behavior with a nearly wide loop compared to other nano superparamagnetic materials, nevertheless, the sample can be considered as soft material with respect to literature[23]. The magnetization saturation (M_s) and remanence magnetization (M_r), are considered as relatively small values but reasonable coercivity (H_c). This result is in accordance with the result published study [24] for the iron sulfides sample which it had a higher M_s. This related to the contribution of each phase to the magnetization, and the contribution of particle size, where, as the particle size is get smaller as M_s get lower [25]. The sample components, Fe_7S_8 and FeO_2 phases, have a relatively low M_s compared to Fe_3S_4 component [26]. This explains the reason behind the low M_s and M_r values besides the low particle size. Despite that, still, the prepared sample still has M_s value larger than that in [27]. The coercivity (H_c) value is lower than that of previous studies[28,26]. The main effective component to H_c is Fe_7S_8 [29].

Magnetic nanoparticles with high M_s are required for hyperthermia applications, where higher M_s lead to larger thermal energy dissipation in the tumor cells. On the other hand, Large M_s values provide more control over the magnetic nanoparticles' mobility in the blood when an external magnetic field is applied [30]. Therapeutic magnetic hyperthermia requires a low M_r, a low field to reach the magnetic saturation, and an ability to regulate the threshold heating temperature [31].

The ultra-high SLP is produced by strong coercivity. Based on that, the ferrimagnetic materials with a significant coercivity are heated up very well in magnetic hyperthermia applications. In current work H_c is relatively high, so it can guess to obtain good SLP for our samples.

The hyperthermic efficiency was estimated by evaluating the specific loss power (SLP) using eq.(2). This quantity was calculated by estimating the slope of temperature raising (T) versus time (t), i.e. ($\triangle T/\triangle t$), of the fitting line in Fig.(5). The SLP value equals to (3548W/g). This value confirms that the synthesized iron sulfide nanoparticles possess an intrinsic magnetic moment that can be stimulated by the externally applied alternating magnetic field to create heat through relaxation processes [32,33]. Since the mean particle size of sample is 36 .24nm, as shown from FESEM analysis, which is near the single domain size, and the particles were hardly dispersed in water, so, It is believed there are no Brownian or Neel relaxation losses contributing to the measured SLP [34], and just hysteresis losses contribute to SLP.

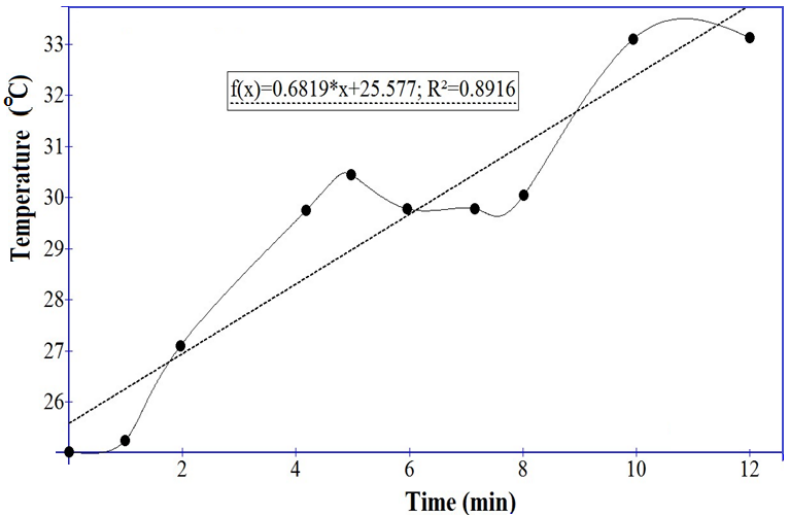

Fig.(5). The temperature variation of iron sulfide suspension in distilled water versus time under AC-magnetic fields.

Conclusions

The magnetic properties of the hydrothermally prepared sample are affected by the components of the phases especially the griegite phase quantity, which in turn affect the hyperthermia and heating up the suspension. Such SLP value is considered as good value compared to literature at such operating parameter of concentration and frequency. The produced particle size by this preparation method and under the mentioned condition is suitable for producing SLP resulted from magnetic hysteresis loss. This SLP can be enhanced more to reach a nearly perfect value operating the suspension at higher frequency and higher concentrations.

References

[1] Zhang, X., Xi, Z., Machuki, J. O. A., Luo, J., Yang, D., Li, J., ... & Gao, F. (2019). Gold cube-in-cube based oxygen nanogenerator: a theranostic nanoplatform for modulating tumor microenvironment for precise chemo-phototherapy and multimodal imaging. *ACS nano*, *13*(5), 5306-5325.

[2] Marzi, M., Osanloo, M., Vakil, M. K., Mansoori, Y., Ghasemian, A., Dehghan, A., & Zarenezhad, E. (2022). Applications of metallic nanoparticles in the skin cancer treatment. *BioMed Research International*, *2022*.

[3] Borghei, Y. S., Hosseinkhani, S., & Ganjali, M. R. (2022). Engineering in modern medicine using 'magnetic nanoparticles' in understanding physicochemical interactions at the nano–bio interfaces. *Materials Today Chemistry*, *23*, 100733

[4] Gautam, S., Bansal, D., Bhatnagar, D., Sharma, C., & Goyal, N. (2023). Synthesis of iron-based nanoparticles by chemical methods and their biomedical applications. In *Oxides for Medical Applications* (pp. 167-195). Woodhead Publishing.

[5] Ibrahim Khan, K. S., & Khan, I. (2019). Nanoparticles: Properties, applications and toxicities. *Arabian journal of chemistry*, *12*(7), 908-931..

[6] Gu, N., Zhang, Z., & Li, Y. (2022). Adaptive iron-based magnetic nanomaterials of high performance for biomedical applications. *Nano Research*, *15*(1), 1-17.

[7] Beković, M., Ban, I., Drofenik, M., & Stergar, J. (2023). Magnetic Nanoparticles as Mediators for Magnetic Hyperthermia Therapy Applications: A Status Review. *Applied Sciences*, *13*(17), 9548.

[8] Farzin, A., Etesami, S. A., Quint, J., Memic, A., & Tamayol, A. (2020). Magnetic nanoparticles in cancer therapy and diagnosis. *Advanced healthcare materials*, *9*(9), 1901058..

[9] Zamani Kouhpanji, M. R., & Stadler, B. J. (2020). A guideline for effectively synthesizing and characterizing magnetic nanoparticles for advancing nanobiotechnology: A review. *Sensors*, *20*(9), 2554.

[10] Liu, X., Zhang, Y., Wang, Y., Zhu, W., Li, G., Ma, X., ... & Liang, X. J. (2020). Comprehensive understanding of magnetic hyperthermia for improving antitumor therapeutic efficacy. *Theranostics*, *10*(8), 3793.

[11] Gan, Y. X., Jayatissa, A. H., Yu, Z., Chen, X., & Li, M. (2020). Hydrothermal synthesis of nanomaterials. *Journal of Nanomaterials*, *2020*, 1-3.

[12] Wu, W., Wu, Z., Yu, T., Jiang, C., & Kim, W. S. (2015). Recent progress on magnetic iron oxide nanoparticles: synthesis, surface functional strategies and biomedical applications. *Science and technology of advanced materials*, *16*(2), 023501.

[13] Y. Duan and J. Sun, "Preparation of Iron-Based Sulfides and Their Applications in Biomedical Fields," *Biomimetics*, vol. 8, no. 2, 2023, doi:

10.3390/biomimetics8020177.

[14] M. Beković, I. Ban, M. Drofenik, and J. Stergar, “Magnetic Nanoparticles as Mediators for Magnetic Hyperthermia Therapy Applications: A Status Review,” *Appl. Sci.*, vol. 13, no. 17, 2023, doi: 10.3390/app13179548.

[15] L. P. Mona, S. P. Songca, and P. A. Ajibade, “Synthesis and encapsulation of iron oxide nanorods for application in magnetic hyperthermia and photothermal therapy,” *Nanotechnol. Rev.*, vol. 11, no. 1, pp. 176–190, 2021, doi: 10.1515/ntrev-2022-0011.

[16] R. A. Revia and M. Zhang, “Magnetite nanoparticles for cancer diagnosis, treatment, and treatment monitoring: Recent advances,” *Mater. Today*, vol. 19, no. 3, pp. 157–168, 2016, doi: 10.1016/j.mattod.2015.08.022.

[17] A. Bhardwaj, K. Parekh, and N. Jain, “In vitro hyperthermic effect of magnetic fluid on cervical and breast cancer cells,” *Sci. Rep.*, vol. 10, no. 1, pp. 1–13, 2020, doi: 10.1038/s41598-020-71552-3.

[18] M. Kallumadil, M. Tada, T. Nakagawa, M. Abe, P. Southern, and Q. A. Pankhurst, “Suitability of commercial colloids for magnetic hyperthermia,” *J. Magn. Magn. Mater.*, vol. 321, no. 10, pp. 1509–1513, 2009, doi: https://doi.org/10.1016/j.jmmm.2009.02.075.

[19] J. D. Bettina Kozissnik Ana C. Bohorquez and C. Rinaldi, “Magnetic fluid hyperthermia: Advances, challenges, and opportunity,” *Int. J. Hyperth.*, vol. 29, no. 8, pp. 706–714, 2013, doi: 10.3109/02656736.2013.837200.

[20] G. Guan *et al.*, “‘Transformed’ Fe3S4 tetragonal nanosheets: a high-efficiency and body-clearable agent for magnetic resonance imaging guided photothermal and chemodynamic synergistic therapy,” *Nanoscale*, vol. 10, no. 37, pp. 17902–17911, 2018, doi: 10.1039/C8NR06507A.

[21] J. Moore, E. Nienhuis, M. Ahmadzadeh, and J. McCloy, “Synthesis of greigite (Fe3S4) particles via a hydrothermal method,” *AIP Adv.*, vol. 9, no. 3, 2019, doi: 10.1063/1.5079759.

[22] Y. H. Chen *et al.*, “Using the high-temperature phase transition of iron sulfide minerals as an indicator of fault slip temperature,” *Sci. Rep.*, vol. 9, no. 1, pp. 1–6, 2019, doi: 10.1038/s41598-019-44319-8.

[23] A. V. Volik, E. A. Pecherskaya, Y. A. Varenik, T. O. Zinchenko, D. V. Artamonov, and O. A. Timohina, “Metrological aspects of an automated method for measuring electrophysical parameters of soft magnetic materials,” *J. Phys. Conf. Ser.*, vol. 2086, no. 1, 2021, doi: 10.1088/1742-6596/2086/1/012072.

[24] Vanitha, P. V., & O'Brien, P. (2008). Phase control in the synthesis of magnetic iron sulfide nanocrystals from a cubane-type Fe− S cluster. *Journal of the American Chemical Society*, *130*(51), 17256-17257.

[25] Lafta, S. H. (2017). The relation of crystallite size and Ni 2+ content to ferromagnetic resonance properties of nano nickel ferrites. *Journal of Magnetics*, *22*(2), 188-195.

[26] Horng, C. S. (2018). Unusual magnetic properties of sedimentary pyrrhotite in methane seepage sediments: Comparison with metamorphic pyrrhotite and sedimentary greigite. *Journal of Geophysical Research: Solid Earth*, *123*(6), 4601-4617.

[27] Streltsov, S. S., Shorikov, A. O., Skornyakov, S. L., Poteryaev, A. I., & Khomskii, D. I. (2017). Unexpected 3+ valence of iron in FeO2, a geologically important material lying "in between" oxides and peroxides. *Scientific reports*, *7*(1), 13005.

[28] Kars, M., & Kodama, K. (2015). Rock magnetic characterization of ferrimagnetic iron sulfides in gas hydrate-bearing marine sediments at Site C0008, Nankai Trough, Pacific Ocean, off-coast Japan. *Earth, Planets and Space*, *67*, 1-12.

[29] Chun-Rong, L., Yaw-Teng, T., & Kun-Yauh, S. (2017). Iron sulfide nanoparticles: preparation, structure, magnetic properties. *Журнал Сибирского федерального университета. Математика и физика*, *10*(2), 244-247.

[30] Obaidat, I. M., Issa, B., & Haik, Y. (2015). Magnetic properties of magnetic nanoparticles for efficient hyperthermia. *Nanomaterials*, *5*(1), 63-89.

[31] Pimentel, B., Caraballo-Vivas, R. J., Checca, N. R., Zverev, V. I., Salakhova, R. T., Makarova, L. A., ... & Reis, M. S. (2018). Threshold heating temperature for magnetic hyperthermia: Controlling the heat exchange with the blocking temperature of magnetic nanoparticles. *Journal of Solid State Chemistry*, *260*, 34-38.

[32] Lemine, O. M., Algessair, S., Madkhali, N., Al-Najar, B., & El-Boubbou, K. (2023). Assessing the Heat Generation and Self-Heating Mechanism of Superparamagnetic Fe3O4 Nanoparticles for Magnetic Hyperthermia Application: The Effects of Concentration, Frequency, and Magnetic Field. *Nanomaterials*, *13*(3), 453.

[33] Maier-Hauff, K., Ulrich, F., Nestler, D., Niehoff, H., Wust, P., Thiesen, B., ... & Jordan, A. (2011). Efficacy and safety of intratumoral thermotherapy using magnetic iron-oxide nanoparticles combined with external beam radiotherapy on patients with recurrent glioblastoma multiforme. *Journal of neuro-oncology*, *103*, 317-324.

[34] Zhang, L. Y., Gu, H. C., & Wang, X. M. (2007). Magnetite ferrofluid with high specific absorption rate for application in hyperthermia. *Journal of Magnetism and Magnetic Materials*, *311*(1), 228-233.